Quark Spectral Functions from Dyson-Schwinger Equations with Spectral Renormalization

Mathieu Kaltschmidt

May 10th, 2021

Institute for Theoretical Physics
University of Heidelberg

This short report summarizes the current state of the art of my Master thesis research carried out as a member of the Strongly Correlated Systems Group at the Institute for Theoretical Physics in Heidelberg under the supervision of Prof. Jan M. Pawlowski.

We compute non-perturbative quark spectral functions for QCD in the Landau gauge. The spectral densities ρ_i are obtained by iteratively solving the corresponding Dyson-Schwinger equation for the quark propagator for a given input gluon spectral function. For the computation of the contributing one-loop quark self energy $\Sigma(p^2)$ we make use of spectral renormalization, a technique based on dimensional regularization which has been developed recently in our group [1–3]. First promising results for the Yang-Mills sector of QCD have successfully proven the power of this method [4]. With our complementary computations for the matter sector of QCD we aim at contributing to the long term goal of our project line: Obtaining a general understanding of the spectral properties of QCD (at finite temperature and density) and its corresponding phase diagram.

1 A Short Introduction and Motivation

A pivotal ingredient in the study of strongly correlated systems are real-time correlation functions since they allow us to access the real-time dynamics of the theory at hand. In the context of QCD this includes for example transport phenomena relevant in the study of heavy-ion collisions [5, 6].

Our theoretical understanding of the non-perturbative sector of QCD has greatly improved during the last decades, mainly due to the complementary efforts and advances in the application of lattice techniques [7, 8] and the application of Functional Methods such as the Functional Renormalization Group (FRG) [9, 10] or Dyson-Schwinger equations (DSEs) [11, 12]. The latter one will be the tool of our choice throughout this work.

Despite the advances in the field, the direct computation of these real-time quantities has turned out to pose several problems. We want to tackle this challenging task by making use of the newly developed technique of spectral renormalization [1–3], allowing for the direct computation of real-time correlation functions from their respective spectral representations.

The next pages serve as a short introduction to the absolute basics needed for a general

understanding of the conducted calculations. The reader familiar with functional methods, the basics of QCD and the Källen-Lehmann spectral representation might skip the remainder of this section in a first read. Note, that in general we will not focus on the technical details but rather try to present the most important conceptual steps of the conducted calculations.

1.1 Functional Methods in Quantum Field Theory

The central object in functional approaches is the quantum effective action $\Gamma[\phi]$, directly related to the generating functional $Z[J]$ via a Legendre transform,

$$\Gamma[\phi] = \sup_J \left\{ \int_x J(x)\phi(x) - W[J] \right\} = \int_x J_{\text{sup}}(x)\phi(x) - W\left[J_{\text{sup}}\right], \tag{1}$$

where $W[J] = \ln Z[J]$, the Schwinger functional, the generating functional of the connected correlation functions. $\Gamma[\phi]$ generates the one-particle irreducible (1PI) correlation functions via functional derivatives w. r. t. the fields, i. e.

$$\Gamma^{(n)}[\phi](p_1, \ldots, p_n) = \frac{\delta^n \Gamma[\phi]}{\delta\phi(p_1) \cdots \delta\phi(p_n)}. \tag{2}$$

Here we presented the momentum space expression. The most important quantity for various applications of functional methods is the field-dependent propagator, given by the inverse of the 1PI two-point function,

$$G[\phi](p, q) = \frac{1}{\Gamma^{(2)}}[\phi](p, q). \tag{3}$$

The path integral measure of the generating functional is invariant under field independent spacetime translations $\phi(x) \to \phi(x) + \Lambda(x)$ and so are the respective correlation functions. The corresponding symmetry identity derived from this is given by

$$\frac{\delta\Gamma[\phi]}{\delta\phi(x)} = \frac{\delta S[\phi]}{\delta\varphi(x)} \left[\varphi = G \cdot \frac{\delta}{\delta\phi} + \phi\right]. \tag{4}$$

This is the famous Dyson-Schwinger equation (DSE), the central functional relation in the context of our work. More formal derivations can for example be found in [13, 14]. Here, $S[\phi]$ is the classical action of the theory at hand, $\phi = \langle\varphi\rangle$ and

$$G \cdot \frac{\delta}{\delta\phi} = \int \frac{\mathrm{d}^d q}{(2\pi)^d} G(p, q) \frac{\delta}{\delta\phi}. \tag{5}$$

This explains how we can extract the correlation functions from the DSE, i. e. by taking functional derivatives of equation (4). The two-point function is therefore obtained by taking a single field derivative. For the quark propagator in QCD, we depict the corresponding one-loop equation in the typical diagrammatic notation in Figure 1 at the beginning of
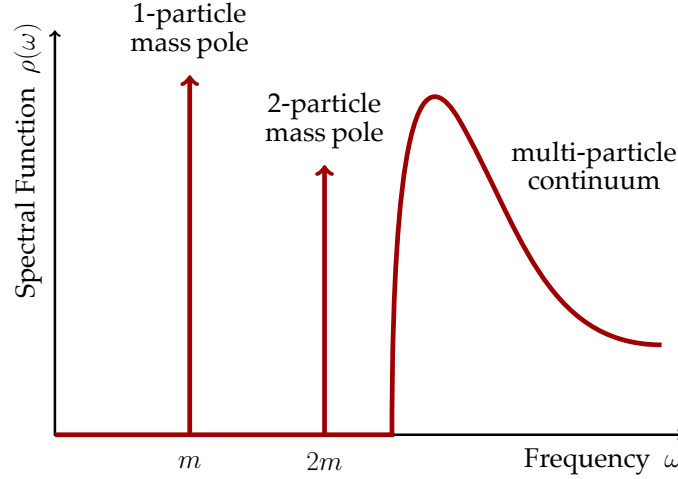
Figure 1: Diagrammatic representation of the quark propagator DSE. Green blobs indicate full propagators, red blobs full vertices and black dots the respective classical counterparts.

the next page. It relates the full (inverse) two-point function to the bare propagator plus higher loop order diagrams, in our case the one-loop quark self energy $\Sigma(p^2)$.

1.2 Relevant Basics of Quantum Chromodynamics

Quantum Chromodynamics, the theory of strong interactions, is formulated as a $SU(N_c)$ gauge theory, where N_c refers to the number of colors. The relevant action functional $S_{\mathrm{QCD}}[\phi]$ for QCD in the Landau gauge reads

$$S_{\mathrm{QCD}}[\phi] = \frac{1}{4} \int_x \left\{ F_{\mu\nu}^a F_{\mu\nu}^a + \frac{1}{2\xi} \left(\partial_\mu A_\mu^a \right)^2 - \bar{c}^a \partial_\mu D_\mu^{ab} c^b + \bar{q} \left(i\slashed{D} + m_q \right) q \right\}, \qquad (6)$$

with the usual conventions for the non-Abelian field strength $F_{\mu\nu} = F_{\mu\nu}^a T^a$ with the generators of the gauge group $T^a \in SU(N_c)$ and

$$F_{\mu\nu}^a = \partial_\mu A_\nu^a - \partial_\nu A_\mu^a + g f^{abc} A_\mu^b A_\nu^c. \qquad (7)$$

Here f^{abc} are the structure constants, g is the strong coupling constant and A_μ^a is the gluon field. The other terms are the usual gauge fixing term with gauge fixing parameter ξ, the ghost term with the ghost and anti-ghost fields c^a and $\bar{c}^a$ and the Dirac or matter part consisting of the fermionic quark and anti-quark fields q and $\bar{q}$ and the respective covariant derivatives and mass terms. A summary of the Feynman rules following from the given action can be for example found on the appendix of [13]. Landau gauge is achieved by the choice $\xi \to 0$. This gauge choice is particularly useful since it allows for a decoupling and closure of the system of all the transverse correlation functions. The pure gauge, or Yang-Mills sector of QCD is currently studied in our group using the same methods as presented here, first results have been published just recently [4].

1.3 Källen-Lehmann Spectral Representation

The Källen-Lehmann spectral representation [15, 16] allows us the recast the propagator, or more general arbitrary correlation functions, in terms of a spectral integral over the

Figure 2: Shape of a typical spectral function of a scalar theory. The isolated poles of the propagator show up as delta peaks in the spectral function. The continuous tail is generated by branch cuts. The visualization is inspired by [13].

respective spectral function $\rho(\lambda)$ with spectral parameter λ[1] as follows:

$$G(p) = \int_0^\infty \frac{\mathrm{d}\lambda}{\pi} \frac{\lambda \rho(\lambda)}{p^2 + \lambda^2}. \tag{8}$$

This can be interpreted as an integral over classical free propagators of a particle with squared mass λ^2 weighted by the spectral density $\rho(\lambda)$, or for the case of asymptotic states, as probability density for the transition to an excited state with energy λ. The spectral density $\rho(\lambda)$ encodes all the information about the energy spectrum of the theory. An example spectral function in the context of a scalar theory is visualized in Figure 2.

In terms of a mathematical interpretation, the spectral function arises as the set of non-analycities of the propagator, whose locations in the complex plane are restricted by Cauchy's theorem. From this an inverse relation between the retarded propagator and the spectral function can be derived. It reads

$$\rho(\omega, |\vec{p}|) = 2 \operatorname{Im}\left[G\left(-i(\omega + i0^+), |\vec{p}|\right) \right], \tag{9}$$

with ω being the zero component of the real-time momentum. Note, that due to the requirement of Lorentz invariance we do not need to consider the spatial momentum explicitly since all kinetic information can be restored from Lorentz invariance. Hence will we drop it for the remainder of this work. This relation is of particular importance, since we will use it later on to extract the spectral function from the computed retarded propagator.

---

1. Note that we choose to work with the convention of a spectral function of a linear argument λ instead of λ^2 which is often found in the literature. This is achieved simply by changing the integration variable from $\mathrm{d}\lambda^2 \to \lambda \, \mathrm{d}\lambda$.

From equations (8) and (9) it follows straightforwardly, that all the non-analycities of the propagator are restricted to the real momentum axis. This allows us to split the spectral function into pole contributions and a continuous (scattering) part generated by branch cuts, i.e.

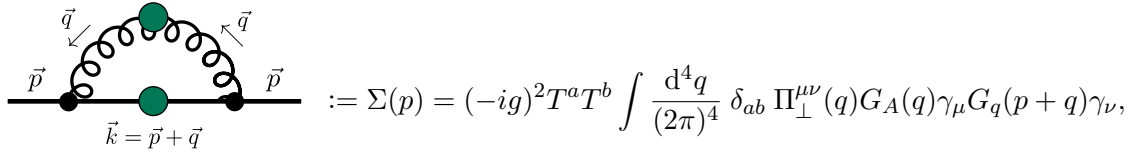$$\rho(\lambda) = \frac{\pi}{\lambda} \sum_i Z_i \, \delta(\lambda - m_i) + \rho_{\text{cont}}(\lambda). \tag{10}$$

From this ansatz the spectral function reproducing the classical propagator is simply obtained from equation (10) by setting $Z_1 = 1$, $Z_{i>1} = 0$ and $\rho_{\text{cont}} = 0$.

With this relatively simple structure at hand we can now move on to the explicit details of the conducted computations. The next section is denoted to the introduction of the important features of the spectral renormalization scheme.

2 Methodology and Spectral Renormalization

We do not state explicit expressions for the integrands here at any point since they are relatively long and complex and not needed for a general understanding of the procedure.

The starting point for our calculation is the one-loop contribution to the quark propagator DSE, the quark self energy diagram. In a first approach we simplify the calculation by working in a classical vertex approximation, i.e. we set $\Gamma^{(3)} \equiv S^{(3)}$. Following QCD Feynman rules in the Landau gauge [13], the diagram then reads

$$:= \Sigma(p) = (-ig)^2 T^a T^b \int \frac{\mathrm{d}^4 q}{(2\pi)^4} \, \delta_{ab} \, \Pi_\perp^{\mu\nu}(q) G_A(q) \gamma_\mu G_q(p+q) \gamma_\nu,$$

with the transverse projection operator

$$\Pi_\perp^{\mu\nu}(p) = \delta^{\mu\nu} - \frac{p^\mu p^\nu}{p^2}, \tag{11}$$

and the spectral representations of the gluon propagator

$$G_A(p) = \int_0^\infty \frac{\mathrm{d}\lambda_A}{\pi} \frac{\lambda_A \rho_A(\lambda_A)}{p^2 + \lambda_A^2}, \tag{12}$$

and the quark propagator

$$G_q(p^2) = \not{p} \int_0^\infty \frac{\mathrm{d}\lambda}{\pi} \frac{\lambda \rho_1(\lambda)}{p^2 + \lambda^2} + \int_0^\infty \frac{\mathrm{d}\lambda}{\pi} \frac{\lambda \rho_2(\lambda)}{p^2 + \lambda^2}. \tag{13}$$

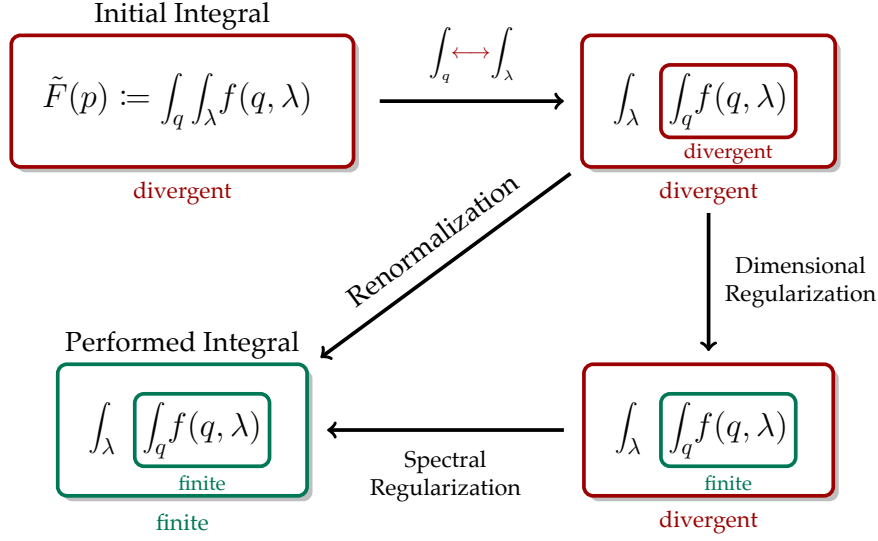Note that the quark propagator is parametrized by two spectral functions, respecting the

Initial Integral

$$\tilde{F}(p) := \int_q \int_\lambda f(q,\lambda)$$

$$\int_q \xleftrightarrow{} \int_\lambda$$

$$\int_\lambda \boxed{\int_q f(q,\lambda)}$$
divergent

divergent

divergent

Renormalization

Dimensional
Regularization

Performed Integral

$$\int_\lambda \boxed{\int_q f(q,\lambda)}$$
finite

finite

$$\int_\lambda \boxed{\int_q f(q,\lambda)}$$
finite

divergent

Spectral
Regularization

Figure 3: Applied regularization procedure. f is some arbitrary divergent integrand. The two upper boxes have to be understood as finite by dimensional regularization but divergent in the limit $\varepsilon \to 0$. The first step consists of evaluating the momentum integral analytically using dimensional regularization before renormalizing the spectral integrands subsequently according to a BPHZ-renormalization scheme.

Dirac structure featuring a Dirac vector part $\sim \not{p}$ and a Dirac scalar part $\sim \mathbb{1}$, where the unit matrix has to be understood as the identity in Dirac space.

In a first step we split the diagram into its vector and scalar component:

$$\Sigma_q(p^2) = \not{p} \cdot \Sigma_{\text{vec}}(p^2) + \mathbb{1} \cdot \Sigma_{\text{scal}}(p^2). \tag{14}$$

Both terms involve two integrations, the usual loop momentum integration and the spectral integration. The integration order is swapped which is only allowed for the case of finite integrands due to Fubinis theorem. A schematic overview on how to renormalize and regularize the respective integrands properly, the spectral renormalization scheme, is presented above in Figure 3. The first task consists in manipulating the occurring tensor structures and momenta such that the momentum integrals can be evaluated analytically using standard formulas known in the context of dimensional regularization, i. e.

$$\int \frac{\mathrm{d}^d q}{(2\pi)^d} \frac{(q^2)^m}{[q^2 + \Delta]^n} = \frac{1}{(4\pi)^{d/2}} \frac{\Gamma(m + \frac{d}{2})\Gamma(n - \frac{d}{2} - m)}{\Gamma(\frac{d}{2})\Gamma(n)} \Delta^{m+d/2-m}, \tag{15}$$

with m a non-negative and n a positive integer [17]. For our computation the relevant expressions have $n = 2$ and $m = 1, 2$. The resulting expressions are evaluated in $d = 4 - 2\varepsilon$ and expanded up to lowest order in $\varepsilon \to 0$. We are left with finite spectral integrands for $\varepsilon > 0$, that in general need to be computed numerically. For numerical performance it is helpful to perform the spectral integrations at $\varepsilon = 0$. The same is true for the access

to the analytical momentum structure needed to extract the Minkowski properties. It is therefore required to set up a suitable renormalization procedure for the integrands in the limit $\varepsilon \to 0$. This means that it is not sufficient to discard the typical $\sim \frac{1}{\varepsilon}$-term after performing the momentum integrals to render the spectral integrands finite, which is a remnant of the swapping of the integration orders in the beginning.

The simplest way of regularizing the spectral integrands is by subtracting terms that render the expressions finite. This can be achieved for example by subtracting a Taylor series of the spectral integrand evaluated at the renormalization scale μ according to the BPHZ-scheme with Dyson's formula.

Note that the BPHZ-scheme in general does not preserve all symmetries of the theory at hand which is the same problem, that occurs when subtracting explicit counterterms in other schemes. The number of terms that need to be subtracted can be determined from naive power counting. Diagrammatically this can be visualized for our case as follows:

$$
\vcenter{\hbox{\includegraphics{d1}}} \;\longrightarrow\; \vcenter{\hbox{\includegraphics{d2}}} \;-\; \vcenter{\hbox{\includegraphics{d3}}}\bigg|_{p=\mu} \;-\; \frac{(p^2 - \mu^2)}{2\mu}\left[\partial_p \; \vcenter{\hbox{\includegraphics{d4}}} \;\right]_{p=\mu}
$$

The counterterms therefore explicitly contribute to the mass renormalization as well as to the wave function renormalization. They consistently remove the divergent parts of the integrands, we explicitly checked for UV-finiteness of all integrations. This finally allows us to solve the spectral integrals numerically after successfully performing the limit $\varepsilon \to 0$ beforehand.

The last step before being able to iteratively extract the spectral functions is the "analytic continuation" to Minkowski spacetime. This is achieved by replacing $p^0 \to -i(\omega + i\varepsilon)$ and taking the limit $\varepsilon \to 0^+$. These integrands can now be used as our input for the numerical evaluation of the spectral integrals, after choosing suitable initial guesses for the spectral functions. More details on the numerical part of this work are presented in the subsequent section.

3   A Few Words on Numerics

The numerical part of the work is performed in Mathematica [18], since it provides all the tools to easily perform manipulations of the spectral integrands, the actual numerical integrations and the iterative procedure.

After computing the spectral integrands $\Sigma_{\mathrm{vec}}(p^2)$ and $\Sigma_{\mathrm{scal}}(p^2)$ and performing the respective spectral regularization as outlined above, we need to make initial guesses for the spectral densities to be able to perform the first iteration step. For the gluon spectral function (cf. Figure 4) we choose a result respecting the so called decoupling (or massive) solution for the gluon propagator in the infrared [19]. This may be adapted later to a
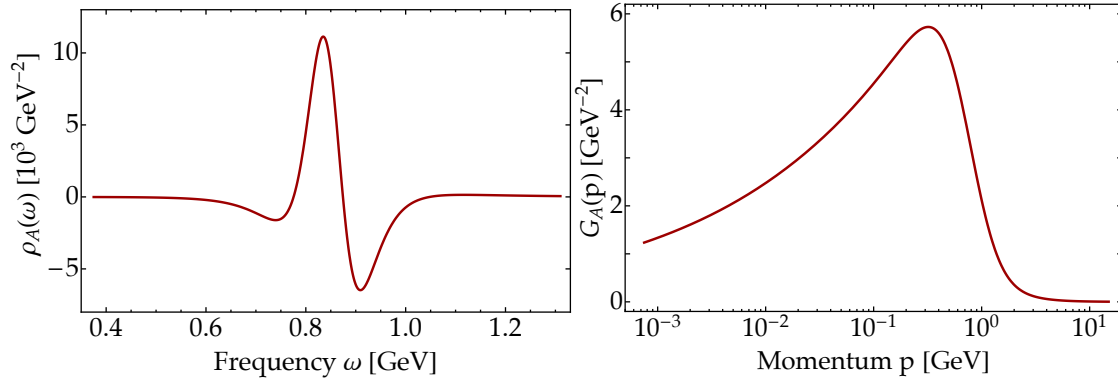
Figure 4: Chosen input gluon spectral function (left) and the corresponding propagator obtained from equation (8) (right). This spectral function was computed by group members using the same techniques, results are not published yet.

solution respecting the known scaling scenario [20], which has been found to provide a dynamical generation of a mass gap for both the gluon and the ghost propagators, but is in general more complicated due to the non-trivial scaling exponent κ with $\frac{1}{2} < \kappa < 1$. For the initial quark spectral functions ρ_1 and ρ_2 we choose the respective "classical" spectral functions, i. e. the ones that reproduce the classical quark propagator:

$$\rho_{1,\text{init}}(\lambda) = 2\pi i \left.\frac{\delta(\lambda - m_q)}{2\lambda}\right|_{\lambda = m_q}$$

$$\rho_{2,\text{init}}(\lambda) = 2\pi m_q \left.\frac{\delta(\lambda - m_q)}{2\lambda}\right|_{\lambda = m_q} . \tag{16}$$

As a final remark in this section we want to show how to explicitly extract the spectral functions ρ_1 and ρ_2 from the retarded quark propagator computed from the DSE. Schematically the inverse quark propagator is parametrized by two scalar dressing functions, i. e.

$$G_q^{-1}(p^2) = i\slashed{p} \cdot A(p^2) + \mathbb{1} \cdot B(p^2) \tag{17}$$

This leaves us with the following expression for the full propagator:

$$G_q(p^2) = -i\slashed{p}\mathcal{A}(p^2; A, B) + \mathcal{B}(p^2; A, B) \equiv \slashed{p}\underbrace{\int_0^\infty \frac{d\lambda}{\pi} \frac{\lambda \rho_1(\lambda)}{p^2 + \lambda^2}}_{\equiv -i\mathcal{A}(p^2)} + \underbrace{\int_0^\infty \frac{d\lambda}{\pi} \frac{\lambda \rho_2(\lambda)}{p^2 + \lambda^2}}_{\equiv \mathcal{B}(p^2)} . \tag{18}$$

Here we identified the respective parts of the propagator with the corresponding parts of the spectral representation (13).
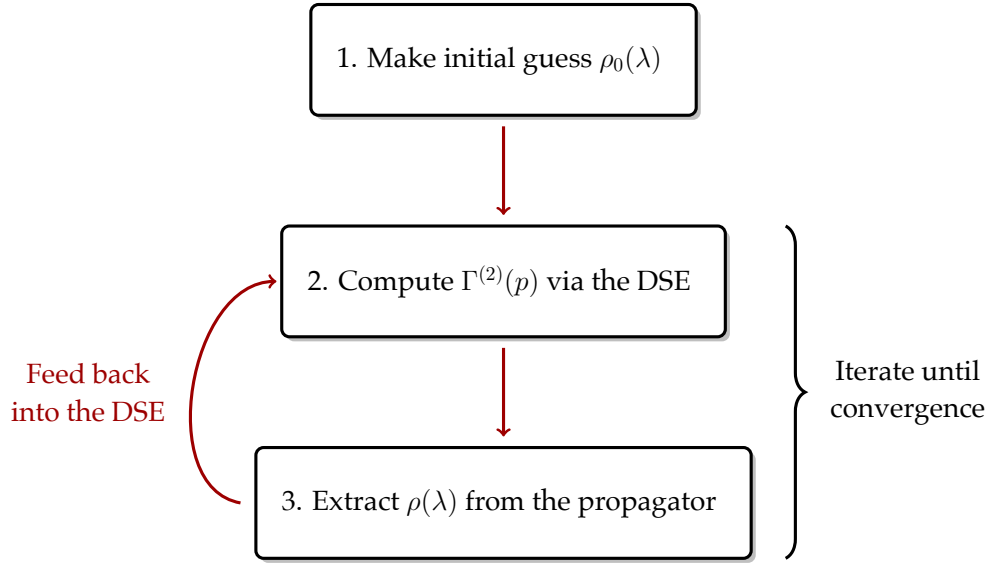
Figure 5: Iterative procedure to extract the spectral function from the inverse propagator obtained from the quark propagator DSE.

The scalar dressings here are related to $A(p^2)$ and $B(p^2)$ via

$$
\mathcal{A}(p^2) = \frac{A(p^2)}{p^2 A^2(p^2) + B^2(p^2)},
$$
$$
\mathcal{B}(p^2) = \frac{B(p^2)}{p^2 A^2(p^2) + B^2(p^2)}.
$$
(19)

With this knowledge at hand, we use equation (9) to find:

$$
\rho_1(\omega) = 2\,\mathrm{Im}\left[\Pi_{\not{p}} G_q\left(-i(\omega + i0^+); \mathcal{A}, \mathcal{B}\right)\right] = 2\,\mathrm{Im}\left[-i\mathcal{A}\left(-i(\omega + i0^+)\right)\right],
$$
$$
\rho_2(\omega) = 2\,\mathrm{Im}\left[\Pi_{\mathbb{1}} G_q\left(-i(\omega + i0^+); \mathcal{A}, \mathcal{B}\right)\right] = 2\,\mathrm{Im}\left[\mathcal{B}\left(-i(\omega + i0^+)\right)\right],
$$
(20)

with the projectors defined such that they allow us to access the relevant parts of the retarded propagator, i. e.

$$
\Pi_{\not{p}}(\cdots) = \mathrm{Tr}_{\mathrm{D}}\left[\frac{\not{p}}{p^2}(\cdots)\right],
$$
$$
\Pi_{\mathbb{1}}(\cdots) = \mathrm{Tr}_{\mathrm{D}}\left[(\cdots)\right].
$$
(21)

Here we used the fact that the trace of an odd number of gamma matrices vanishes. The index D refers to the Dirac trace.

With this initial setup at hand we can start the iteration and stepwise compute the spectral integrations, the Euclidean and real-time version of the scalar dressings of the inverse propagator $A(p^2/\omega^2)$ and $B(p^2/\omega^2)$ and of the full propagator $\mathcal{A}(p^2/\omega^2)$ and $\mathcal{B}(p^2/\omega^2)$ and finally extract the spectral functions for the quarks via equation (20). As an overview, the general structure of our code is visualized in Figure 5.

A mandatory benchmark test for the correctness of the spectral function is of course the direct comparison of the Euclidean quark propagator with the the one obtained from the (updated) spectral function via equation (13).

4 Preliminary Results

Up to now, we finished the computation of the quark self energy diagram and compared those results in the chiral limit $\lambda_i \to 0$ to perturbative results, performed the spectral regularization via the BPHZ-scheme, set up the iteration and performed a few trials. Currently the iteration is updated and finalized to be finally able to extract the spectral functions.

5 Outlook

After finishing the computation in the classical vertex approximation it would be of course desirable to include the full vertex, as it naturally appears in the DSE . This of course complicates the computation, since another spectral representation, i. e. for the quark-gluon vertex, needs to be included in the calculation of the one-loop digram and therefore another spectral integration needs to be performed for every iteration step.

On longer terms, we want to extend our results to finite temperatures and densities. This can for example be examined within thermal field theory approaches such as the Matsubara formalism [21], where the momentum integration in the time domain p^0 is replaced by a discrete sum over the respective Matsubara frequencies, giving rise to the usual quantum statistical distribution functions that directly depend on temperature and chemical potential. This is currently studied in a scalar theory setting in our group.

One possibility for improvements on the numerical side, especially if we wish for faster iteration times, would be to discretize the spectral integrands on a three-dimensional grid (in the $p/\omega - \lambda_A - \lambda$ parameter space) and interpolate the obtained data points using standard routines provided by Mathematica such as Hermite polynomials and B-splines.

Of course, the general aim of our project line is to have a precise knowledge of the spectral properties of all relevant QCD quantities. Once this is achieved, this can be used to study and make predictions for various interesting QCD phenomena such as the dynamics of the quark-gluon plasma in relativistic heavy-ion collisions whose evolution is usually described in terms of hydrodynamical transport equations [5, 6].

Selected References

[1]   Jan Horak. "Spectral Functions from Dyson-Schwinger Equations with Dimensional Regularization". Master thesis. Heidelberg University. 2019.

[2]   Nicolas Wink. "Towards the spectral properties and phase structure of QCD". PhD thesis. Heidelberg University. 2020.

[3]   Jan Horak, Jan M. Pawlowski, and Nicolas Wink. "Spectral functions in the ϕ^4-theory from the spectral DSE". In: (2020). arXiv: 2006.09778 [hep-th].

[4]   Jan Horak et al. "Ghost spectral function from the spectral Dyson-Schwinger equation". In: (2021). arXiv: 2103.16175 [hep-th].

[5]   S. Ayik, W. Norenberg, and Georg Wolschin. "Microscopic transport theory of heavy ion collisions". In: *Z. Phys. A* 286 (1978), pp. 271–279.

[6]   Jun Xu. "Transport approaches for the description of intermediate-energy heavy-ion collisions". In: *Prog. Part. Nucl. Phys.* 106 (2019), pp. 312–359. arXiv: 1904.00131 [nucl-th].

[7]   Owe Philipsen. "Lattice QCD at finite temperature and density". In: *Eur. Phys. J. ST* 152 (2007). Ed. by C. Gattringer and C. B. Lang, pp. 29–60. arXiv: 0708.1293 [hep-lat].

[8]   Philippe de Forcrand. "Simulating QCD at finite density". In: *PoS* LAT2009 (2009). Ed. by Chuan Liu and Yu Zhu, p. 010. arXiv: 1005.0539 [hep-lat].

[9]   Christof Wetterich. "Exact evolution equation for the effective potential". In: *Phys. Lett. B* 301 (1993), pp. 90–94. arXiv: 1710.05815 [hep-th].

[10]   Jan M. Pawlowski. "Aspects of the functional renormalisation group". In: *Annals Phys.* 322 (2007), pp. 2831–2915. arXiv: hep-th/0512261.

[11]   Freeman J. Dyson. "The S Matrix in Quantum Electrodynamics". In: *Phys. Rev.* 75 (11 1949), pp. 1736–1755.

[12]   Julian S. Schwinger. "On the Green's functions of quantized fields. 1+2." In: *Proc. Nat. Acad. Sci.* 37 (1951), pp. 452–455.

[13]   Jan. M. Pawlowski et al. *The Functional Renormalization Group & Applications to Gauge Theories and Gravity*. Lecture Notes (Access currently restricted to students). Heidelberg University. 2021.

[14]   Reinhard Alkofer and Lorenz von Smekal. "The Infrared behavior of QCD Green's functions: Confinement, dynamical symmetry breaking, and hadrons as relativistic bound states". In: *Phys. Rept.* 353 (2001), p. 281. arXiv: hep-ph/0007355.

[15]   Gunnar Kallen. "On the definition of the Renormalization Constants in Quantum Electrodynamics". In: *Helv. Phys. Acta* 25.4 (1952), p. 417.

[16]   H. Lehmann. "On the Properties of propagation functions and renormalization constants of quantized fields". In: *Nuovo Cim.* 11 (1954), pp. 342–357.

[17]   Michael E. Peskin and Daniel V. Schroeder. *An Introduction to Quantum Field Theory*. Reading, USA: Addison-Wesley, 1995.

[18]   Wolfram Research Inc. *Mathematica, Version 12.2*. Champaign, IL, 2020.

[19]   Lorenz von Smekal, Reinhard Alkofer, and Andreas Hauck. "The Infrared behavior of gluon and ghost propagators in Landau gauge QCD". In: *Phys. Rev. Lett.* 79 (1997), pp. 3591–3594. arXiv: hep-ph/9705242.

[20]   Christoph Lerche and Lorenz von Smekal. "On the infrared exponent for gluon and ghost propagation in Landau gauge QCD". In: *Phys. Rev. D* 65 (2002), p. 125006. arXiv: hep-ph/0202194.

[21]   Takeo Matsubara. "A New Approach to Quantum Statistical Mechanics". In: *Prog. Theor. Phys.* 14 (1955), pp. 351–378.